Dark states in the magnetotransport through triple quantum dots

Clive Emary

Institut für Theoretische Physik, Hardenbergstrasse 36, TU Berlin, D-10623 Berlin, Germany

We consider the transport through a system of three coupled quantum dots in a perpendicular magnetic field. At zero field, destructive interference can trap an electron in a dark state—a coherent superposition of dot states that completely blocks current flow. The magnetic field can disrupt this interference, giving rise to oscillations in the current and its higher-order statistics as the field is increased. These oscillations have a period of either the flux-quantum or half the flux quantum, depending on the dot geometry. We give results for the stationary current, and the shot noise and skewness both at zero and finite frequency.

I. INTRODUCTION

The quantum-mechanical interference of electronic paths in a conductor gives rise to a number of interesting phenomena in mesoscopic physics. Perhaps the most familiar is the occurrence of Aharonov-Bohm (AB) oscillations[1] in the current through multiply connected structures in a magnetic field.[2] These oscillations arise due to the accumulation of a phase difference ϕ between different paths through the device given by $\phi = \oint \mathbf{A} \cdot d\mathbf{l} = 2\pi\Phi/\Phi_0$, with Φ as the flux enclosed by the device and $\Phi_0 = h/e$ the magnetic flux quantum.

The period of such oscillations is dependent on the nature of the interfering paths and, therefore, on the specific system in question. Flux periods of Φ_0 are what one expects in conventional AB experiments, such as those on coherent beams of electrons in free space.[3] This period is also frequently encountered in mesoscopic experiments, for example, in normal metal rings[4] and in electronic Mach-Zehnder-style interferometers,[5,6] including those with one[7,8] or two[9] quantum dots in the arms. The flux period $\Phi_0/2$ is also observed, not only in superconducting systems,[10] but also in normal metals[11,12] due to weak-localization effects.[13]

A different quantum-coherent effect was described for mesoscopic systems in Ref. 14—that of coherent population trapping (CPT) in quantum dots. In this all-electronic analog of a quantum optics effect,[15–17] the coupling geometry of a triple quantum dot (QD) leads to the establishment of a so-called "dark state" that completely blocks the current through the device. The dark state is composed of a coherent superposition of electronic states in different dots.

In this paper, we consider the interplay of coherent population trapping and the AB phase. We demonstrate how a magnetic field can destroy the delicate phase canceling that maintains the dark state, lift the current blockade, and give rise to current oscillations as the field increases. Furthermore, we show that in a triple-QD structure, such as in Fig. 1, the oscillations can exhibit periods of both Φ_0 and $\frac{1}{2}\Phi_0$ depending on the symmetry of the system. We give results not only for the stationary current but also for the shot noise and skewness (second and third current cumulants, respectively) both at zero[18] and at finite frequency.[19] We also consider the effect of dephasing on the current oscillations.

We consider the QD geometry depicted in Fig. 1. The AB effect requires that all three dots be coupled in a ring struc-

ture as shown, which is in contrast to Ref. 14, where only two "bonds" were present, and no such effect would be observed. Structures similar to that of Fig. 1 are currently being investigated by several experimental groups.[20–23] We work in the strong Coulomb blockade regime such that there is at most one excess electron in the three-dot system at any one time. Each dot has a single level relevant to transport, and we denote as $|i\rangle$ the state with an electron in dot i. The Hamiltonian in the basis $\{|1\rangle, |2\rangle, |3\rangle\}$ is then

$$\mathcal{H} = \begin{pmatrix} \Delta & t_{12}e^{i\phi} & t_{13} \\ t_{12}e^{-i\phi} & -\Delta & t_{23} \\ t_{13} & t_{23} & \epsilon \end{pmatrix}, \quad (1)$$

where ϵ and Δ describe the energies of the dot levels and t_{ij} are the tunnel couplings. Without magnetic field, time-reversal symmetry means that all t_{ij} are real, and we take them all to be positive. Application of the magnetic field breaks this symmetry, and the amplitudes will be complex in general. We choose a gauge such that the phase $\phi = 2\pi\Phi/\Phi_0$ is accumulated on the bond between dots 1 and 2. Finally, dots 1 and 2 are connected to source leads, and dot 3 to the drain.

The density matrix (DM) for the system $\rho(t)$ contains entries not only for the three single electron states $|i\rangle$, but also for the empty state $|0\rangle$. Within the Born-Markov and infinite-bias approximations, the time evolution of the DM is given by the generalized master equation in the Lindblad form,

$$\frac{d\rho}{dt} = -i[\mathcal{H}, \rho] + \sum_k D_k \rho D_k^\dagger - \frac{1}{2}D_k^\dagger D_k \rho - \frac{1}{2}\rho D_k^\dagger D_k, \quad (2)$$

where the quantum jump operators $D_1 = \sqrt{\Gamma_1}|1\rangle\langle 0|$, $D_2 = \sqrt{\Gamma_2}|2\rangle\langle 0|$, and $D_3 = \sqrt{\Gamma_3}|0\rangle\langle 3|$ describe irreversible tunneling of electrons into and out of the system with rates Γ_i. In the following, we set all these rates equal: $\Gamma_i = \Gamma$.

Starting from initial DM $\rho(0) = |0\rangle\langle 0|$, the DM at subsequent time has ten nonzero elements if we assume the most general parameters in $\mathcal{H}$. We arrange these elements into the column vector

$$\boldsymbol{\rho}(t) = (\rho_{00}, \rho_{11}, \rho_{22}, \rho_{33}, \Im\rho_{12}, \Im\rho_{13}, \Im\rho_{23}, \Re\rho_{12}, \Re\rho_{13}, \Re\rho_{23})^T.$$

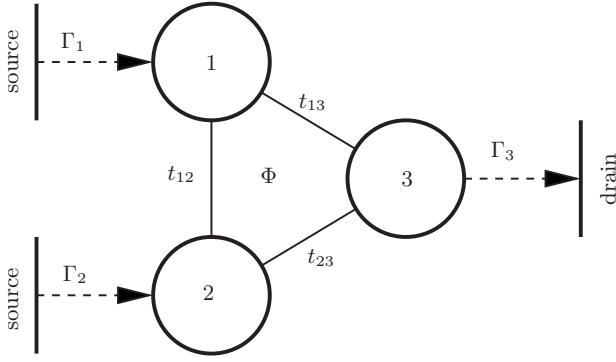The master equation [Eq. (2)] can then be written as

FIG. 1. Three quantum dots are coupled coherently to one another via tunnel couplings t_{ij} and incoherently to source and drain leads with rates Γ_i. Each dot contains a single level and by adjusting the relative positions of these levels, the system can be prepared in a dark state where no current flows despite the applied bias. In a perpendicular magnetic field, the structure encloses a magnetic flux Φ, which causes a phase difference between different paths around the system that can disrupt the dark state and lead to current flow.

$$\dot{\rho} = \mathcal{L}\rho, \qquad (3)$$

with the Liouvillian $\mathcal{L}$ given in the Appendix. The stationary properties of the system are determined by the eigenvalues and eigenvectors of $\mathcal{L}$.[19] The stationary DM, $\rho(\infty)$ is given by the eigenvector of $\mathcal{L}$ with zero eigenvalue, whence the stationary average current $\langle I \rangle = \Gamma \rho_{33}(\infty)$. To calculate higher-order statistics, we require the full spectral decomposition of $\mathcal{L}$.[19] We initially consider the behavior of the system in the absence of dephasing and return to its effects later.

II. ZERO-FIELD CURRENT

We first consider the properties of the system at zero magnetic field ($\phi=0$). In Ref. 14, it was shown that, with the special choice of parameters $t_{12}=0$, $\epsilon=\Delta=0$, and $t_{13}=t_{23}$, the system always reaches the trapped pure state $|\Psi\rangle=(|1\rangle-|2\rangle)/\sqrt{2}$ in the stationary limit (in the absence of dephasing). This exact parameter set is unlikely to pertain to experiment, and it is important to show the existence of the dark state for more general parameters.

If we set $\Delta = \Delta_0$, with

$$\Delta_0 \equiv \frac{t_{12}}{2t_{13}t_{23}}(t_{13}^2 - t_{23}^2), \qquad (4)$$

then, as can easily be verified, the state

$$|\Psi_{\text{dark}}\rangle = \frac{1}{\sqrt{t_{13}^2 + t_{23}^2}}(t_{23}|1\rangle - t_{13}|2\rangle) \qquad (5)$$

is an eigenstate of Hamiltonian (1). Moreover, the vector corresponding to the pure DM

$$\rho_{\text{dark}} = |\Psi_{\text{dark}}\rangle\langle\Psi_{\text{dark}}| \qquad (6)$$

is the eigenvector of $\mathcal{L}$ with eigenvalue zero, and thus ρ_{dark} is the stationary state of the system. Since this state has no electronic density at the drain dot (dot 3), the stationary cur-
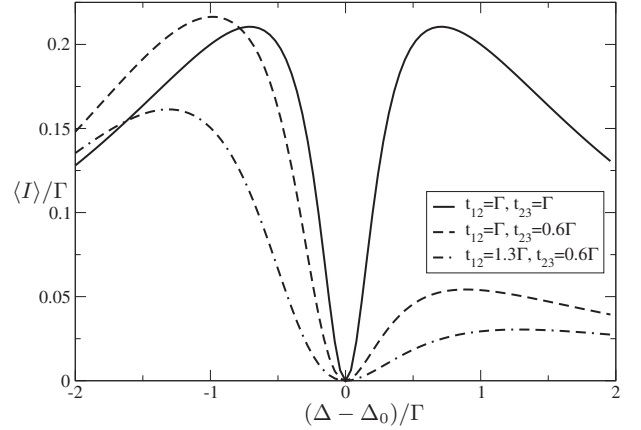

FIG. 2. At zero field, the stationary current $\langle I \rangle$ through the three-dot system shows a pronounced antiresonance with complete current blocking at a detuning of $\Delta=\Delta_0$, where the dark-state forms. The three curves show the current for different values of the coupling parameters (t_{12}, t_{23}), with $t_{13}=\Gamma$ in each case. At zero field, a dark state always exists whenever both t_{13} and t_{23} are finite.

rent through the device is exactly zero. If we assume, therefore, that we have experimental control of the detuning Δ by, for example, backgates under the dots, then a dark state can always be found at zero field by sweeping Δ. It should be noted that the detuning ϵ does not affect the existence of the dark state.

A special instance of our geometry is when $t_{23}=t_{13}$ such that, in the absence of magnetic field, the system is symmetric under the exchange of dots 1 and 2. We will refer to this situation as the "symmetric" case in what follows. In this case, the dark state forms at $\Delta=0=\Delta_0$ and the system permits exact solutions.

In this symmetric case at zero field with $\epsilon=0$ and Δ, a freely variable parameter, we have for the stationary current

$$\langle I \rangle = \frac{4\Gamma\Delta^2 t_{13}^2}{4\Delta^4 + \Gamma^2 t_{12}^2 + 4(t_{13}^2 - t_{12}^2)^2 + \Delta^2(\Gamma^2 + 6t_{13}^2 + 8t_{12}^2)}.$$

Figure 2 shows the stationary current through the device for $B=0$ as a function of the detuning Δ. We show not only the result for the symmetric case, but also numerical results for various asymmetric couplings. In each case, an antiresonance occurs with complete current suppression at $\Delta=\Delta_0$. Unless otherwise stated, we will always set $\Delta=\Delta_0$ in the following, such that there is CPT at zero field.

III. CURRENT OSCILLATIONS

The application of magnetic field has the capacity to lift the dark-state current blockade and give rise to oscillations in the current. In the symmetric case, an exact expression for the current at finite field can be found. With $\epsilon=0$, we have

$$\langle I \rangle(\phi) = \frac{4\Gamma t_{13}^2 t_{12}^2 \sin^2\phi}{4(t_{12}^4 + t_{13}^4) + t_{12}^2[\Gamma^2 - t_{13}^2(1 + 7\cos 2\phi)]}, \qquad (7)$$

which is plotted in Fig. 3. The current shows clear oscillations with superconducting flux period $\frac{1}{2}\Phi_0$. We will return
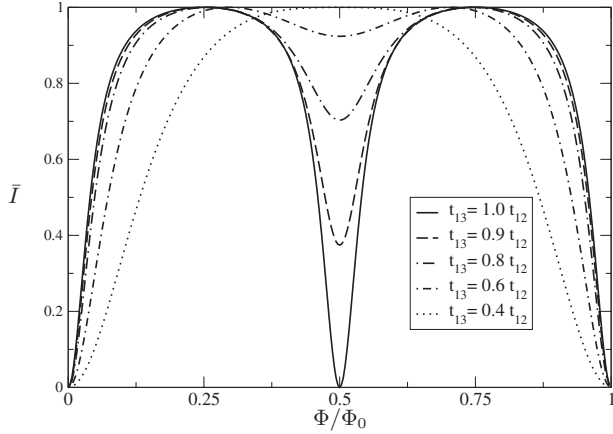
FIG. 3. The stationary current through the three-dot system shows pronounced oscillations as a function of the applied flux. Plotted here is $\bar{I}=\langle I\rangle/\langle I\rangle_{\max}$, the ratio of the current to its maximum value, which always occurs at $\Phi=\frac{1}{4}\Phi_0$. The different curves are for different values of t_{13}. Other parameters were $t_{12}=t_{23}=\Gamma$, $\epsilon=0$, and $\Delta=\Delta_0$, such that CPT occurs at zero field. In the symmetric case with $t_{13}=t_{23}$ (solid curve), CPT trapping occurs at $\frac{n}{2}\Phi_0$, $n=0,1,2,\ldots$, and the flux period of the oscillations is thus $\frac{1}{2}\Phi_0$. As t_{13} moves away from symmetry, the dark-state current blocking at $\frac{n}{2}\Phi_0$, odd n disappears, and the period of the oscillations doubles to Φ_0.

to a discussion of which paths interfere here in a moment. Let us first note that the maximum current as a function of Φ occurs at $\Phi=\frac{1}{4}\Phi_0$, irrespective of t_{12}, and that the current at this value of Φ is itself maximized by setting $t_{12}=t_{13}$. With this choice, the current in the weak coupling limit $t_{13}\ll\Gamma$ is given by $\langle I\rangle=4t_{13}^2/\Gamma\sin^2\phi$, and in the opposite regime, $t_{13}\gg\Gamma$, we have $\langle I\rangle=2\Gamma/7$ for all ϕ except at $n\pi$ where it is exactly zero. This means that the oscillations are easier to observe in the weak coupling limit.

The suppression of the current at $\Phi=\pm\frac{n}{2}\Phi_0$, with odd n, is a consequence of the additional symmetry of the above situation. Figure 3 also shows the behavior of the current as we move away from the symmetric coupling. As the asymmetry increases, the features at odd multiples of $\frac{1}{2}\Phi_0$ disappear, doubling the period of the oscillations to Φ_0. Setting $t_{23}=t_{12}$ and $t_{13}=t_{12}(1+\alpha)$, a perturbation series for the current in α away from the symmetric case shows the current at $\Phi=\frac{1}{2}\Phi_0$ to be

$$\langle I\rangle = 16t_{12}^2\alpha^2/\Gamma + O(\alpha^4). \tag{8}$$

That this dependence is quadratic suggests that some degree of current suppression at odd multiples of $\frac{1}{2}\Phi_0$ may be visible in experiment.

The above results can be understood by consideration of the interference between different paths around the dots. Consider the three-dot system to be occupied and isolated from the leads. If we assume that at time $\tau=0$ the system is in the pure state $|\Psi(0)\rangle$, then the wave function at later time τ is $|\Psi(t)\rangle=e^{-i\mathcal{H}t}|\Psi(0)\rangle$ which, for small times, can be expanded as $|\Psi(t)\rangle\approx\left(1-i\tau\mathcal{H}-\frac{1}{2}\tau^2\mathcal{H}^2\right)|\Psi(0)\rangle$. Consider system initially in the state $|1\rangle$. To first order in τ, evolution

under the full Hamiltonian with $\Delta=\Delta_0$ gives $\mathcal{H}|1\rangle=\Delta_0|1\rangle+t_{12}e^{-i\phi}|2\rangle+t_{13}|3\rangle$. Therefore, the first-order amplitude for the transmission from dot 1 to 3 is $a_{31}^{(1)}=\langle 3|\mathcal{H}|1\rangle=t_{13}$. Similarly, the amplitude from dot 2 to 3 is $a_{32}^{(1)}=\langle 3|\mathcal{H}|2\rangle=t_{23}$. Thus, if we start the system in the dark-state superposition $|\Psi\rangle=1/N(t_{23}|1\rangle-t_{13}|2\rangle)$, with norm $N=\sqrt{t_{23}^2+t_{13}^2}$, these two paths interfere destructively at dot 3 with a total amplitude of $a_{3\Psi}^{(1)}=\langle 3|\mathcal{H}|\Psi\rangle=(t_{23}a_{31}^{(1)}-t_{13}a_{32}^{(1)})/N=0$. The dark state is therefore stabilized against first-order tunneling regardless of the applied field.

The unblocking of the system at a finite B field occurs at second order. Consider the second-order amplitude from dot 1 to 3:

$$a_{31}^{(2)} = \frac{1}{2}\langle 3|\mathcal{H}^2|1\rangle$$

$$= \frac{1}{2}\sum_{i=1}^{3}\langle 3|\mathcal{H}|i\rangle\langle i|\mathcal{H}|1\rangle = \frac{1}{2}(\Delta_0 t_{13} + \epsilon t_{13} + e^{-i\phi}t_{12}t_{23}), \tag{9}$$

which has contributions from the three paths 113, 123, and 133. Similarly, the three paths 223, 233, and 213 give the second-order amplitude from dot 2 to 3 as

$$a_{32}^{(2)} = \frac{1}{2}(-\Delta_0 t_{23} + \epsilon t_{23} + e^{i\phi}t_{12}t_{13}). \tag{10}$$

The total second-order amplitude for the dark-state electron to tunnel to dot 3 is then

$$a_{3\Psi}^{(2)} = \frac{1}{2N^2}t_{12}(e^{-i\phi}-1)(e^{i\phi}t_{13}^2 + t_{23}^2), \tag{11}$$

and the corresponding probability $p^{(2)}=\tau^2|a^{(2)}|^2$ is

$$p^{(2)} = \frac{\tau^2}{2N^4}t_{12}^2(1-\cos\phi)(t_{13}^4 + t_{23}^4 + 2t_{13}^2 t_{23}^2\cos\phi). \tag{12}$$

We see immediately that this probability is zero at zero field and indeed for any $\Phi=n\Phi_0$, n integer, due to the $(1-\cos\phi)$ factor in the above. This gives rise to the standard AB oscillation period of Φ_0. However, if $t_{13}^2=t_{23}^2$, the probability becomes $p^{(2)}=\frac{1}{4}\tau^2 t_{12}^2\sin^2\phi$, implying current blocking with period $\frac{1}{2}\Phi_0$. This halved oscillation period results from the symmetry of the two paths 123 and 213 when $t_{13}=t_{23}$. To see how this arises, let us consider the case $\Phi=\frac{n}{2}\Phi_0$, and we have the factors $e^{\pm i\phi}=-1$ in the Hamiltonian of Eq. (1). This Hamiltonian also possesses a dark state for arbitrary values of the couplings, provided that we set the detunng $\Delta=-\Delta_0$. This dark is the same as that of Eq. (5), except that the superposition has the opposite sign. This therefore means that setting $\Delta=-\Delta_0$, instead of $\Delta=\Delta_0$, is equivalent to shifting the phase of the current oscillations by ϕ, such that the dark states occur at $\frac{n}{2}\Phi_0$, with odd n. In the special symmetric case with $t_{13}=t_{23}$, we obtain $\Delta_0=0$ from Eq. (4). Therefore, dark states can form at $\frac{n}{2}\Phi_0$ not only with even n but also with odd n as these values alternatively satisfy the criteria $\Delta=\pm\Delta_0$.

IV. DEPHASING

We model the influence of dephasing due to charge noise through the introduction of the three jump operators

$$D_i^\gamma = \sqrt{\gamma}|i\rangle\langle i|, \quad i = 1, 2, 3, \tag{13}$$

which enter in Eq. (2) in the same way as do the jump operators D_i. Out of simplicity, we assume the decoherence rate γ to be the same for each dot, and we give here only results for the case when all three couplings are equal, $t_{ij}=t$. In this case, the current as a function of the phase ϕ and decoherence rate γ is

$$\langle I \rangle(\phi, \gamma) = \frac{\Gamma(4\gamma(\Gamma + 2\gamma)t_{13}^2 + 2f(\phi))}{\Gamma\gamma(\Gamma + 2\gamma)^2 + 2(2\Gamma^2 + 13\Gamma\gamma + 14\gamma^2)t_{13}^2 + 7f(\phi)},$$

with ϕ dependence contained in the function

$$f(\phi) = 8t_{13}^4(\Gamma + 3\gamma)(\Gamma + 2\gamma)^{-1} \sin^2 \phi. \tag{14}$$

Since $f(0)=0$, the dephasing leads to a finite current at zero field through the disruption of the coherence between the two dark-state dots.[14] The effect of dephasing on the oscillations can be quantified through the visibility

$$\nu(\gamma) \equiv 1 - \frac{\langle I \rangle(\phi_{\min}, \gamma)}{\langle I \rangle(\phi_{\max}, \gamma)}. \tag{15}$$

This is found to be

$$\nu(\gamma) = \frac{4\Gamma(\Gamma + 3\gamma)t_{13}^2}{\Gamma\gamma(\Gamma + 2\gamma)^2 + 2t_{13}^2(2\Gamma^2 + 13\Gamma\gamma + 14\gamma^2)}. \tag{16}$$

For small dephasing, $\gamma \ll \Gamma$, the visibility deviates from unity as

$$\nu = 1 - \gamma[(7/2\Gamma) + (\Gamma/4t_{13}^2)] \tag{17}$$

and for strong dephasing $\gamma \gg \Gamma$, we have $\nu = 3t_{13}^2/\gamma^2$.

V. HIGHER-ORDER CURRENT STATISTICS

The dark state and magnetic field also influence the higher statistics of the current through the device. Here, we focus on the second and third current cumulants at both zero and finite frequency. We give results for the two finite-frequency Fano factors: $F^{(2)}(\omega) \equiv S^{(2)}(\omega)/\langle I \rangle$, where $S^{(2)}(\omega)$ is the shot noise and $F^{(3)}(\omega, \omega') \equiv S^{(3)}(\omega, \omega')/\langle I \rangle$ with the skewness

$$S^{(3)}(\omega, \omega') = \int d\tau d\tau' e^{i\omega\tau + i\omega'\tau'} \langle \delta I(0)\,\delta I(\tau)\,\delta I(\tau') \rangle. \tag{18}$$

These quantities can be straightforwardly calculated using the results of Ref. 19 from λ_i, the eigenvalues of $\mathcal{L}$, and V, the corresponding matrix of its eigenvectors. Let $\mathcal{L}_J$ be the jump operator that transfers an electron to the drain from dot 3. In the basis of vector ρ, it has elements $(\mathcal{L}_J)_{ij} = \Gamma\delta_{i1}\delta_{j4}$. The Fano factors can then be expressed solely in terms of the eigenvectors λ_i and the quantities $c_k \equiv (V^{-1}\mathcal{L}_J V)_{kk}$.

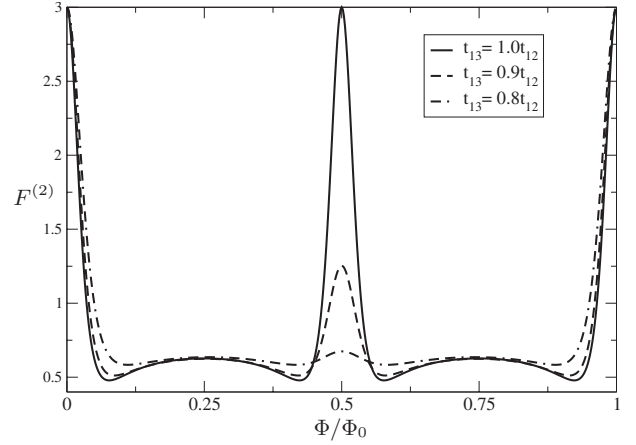The finite-frequency shot noise Fano factor is given by

FIG. 4. The zero-frequency (shot noise) Fano factor $F^{(2)}(0)$ for the three-dot system as a function of magnetic flux also exhibits oscillations. We observe strong super-Poissonian peaks with $F^{(2)}(0)=3$ at the values of flux for which the dark-state forms (Ref. 18). Away from these points, the noise is sub-Poissonian. The period of these oscillations is the same as for the current. Same parameters as for Fig. 3, except for the displayed values of t_{13}.

$$F^{(2)}(\omega) = 1 - 2\sum_k \frac{c_k\lambda_k}{\omega^2 + \lambda_k^2}. \tag{19}$$

The zero-frequency result, $F^{(2)}(0)$, is shown in Fig. 4 as a function of Φ for several couplings. At $\Phi = n\Phi_0$, $n = 0, 1, \ldots$, we see highly super-Poissonian maxima with Fano factor $F^{(2)}(0)=3$, which is the same value as that found for the $t_{12}=0$ model discussed in Ref. 18. In the symmetric case $t_{13}=t_{23}$, we see further maxima at $\Phi = \frac{n}{2}\Phi_0$, also with $F^{(2)}(0)=3$. These latter disappear as the coupling asymmetry increases. In between these sharp super-Poissonian peaks, the shot noise is strongly sub-Poissonian, and we therefore observe considerable variation in systems behavior as the field is changed.

The shot noise Fano factor at finite frequency $F^{(2)}(\omega)$ is shown for symmetric coupling in Fig. 5. We see that the large super-Poissonian peaks occur only close to zero frequency, as the majority of the behavior is sub-Poissonian. Nevertheless, further structure is to be observed at finite frequency, with a number of inflexion points occurring as a function of ω, the locations of which are determined by the spectrum of the isolated Hamiltonian $\mathcal{H}$. The inflexions are located at $\omega = \Delta E_{ij}$, where $\Delta E_{ij} = |E_i - E_j|$ are the differences between all the eigenenergies of $\mathcal{H}$. In the case where all three couplings are equal, these energies are obtained from the three solutions of the equation $E_i^3 - 3t_{13}^2 E_i - 2t_{13}^3 \cos \phi = 0$, and the corresponding differences are shown overlaid on Fig. 5.

The skewness is calculated from an expression similar to Eq. (19), but lengthier. We obtain the zero-frequency result shown in Fig. 6, which has the zero-field limit of $F^{(3)}(0) = 13$, in agreement with Ref. 18. The behavior of the skewness as a function of field strength is similar to that of the shot noise, but here the contrast between the values with and without the dark start is even more pronounced.
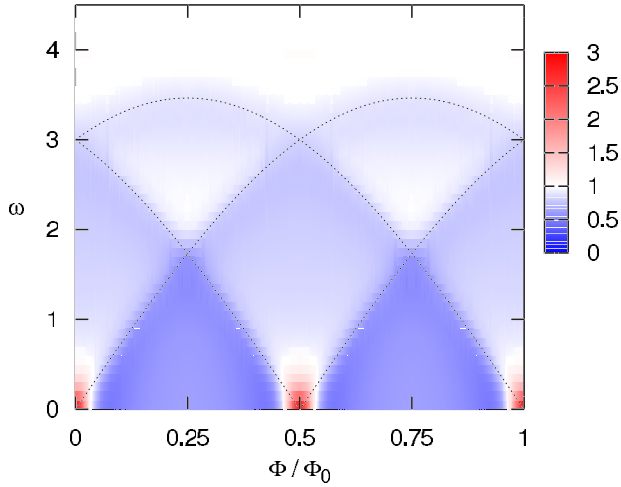
FIG. 5. (Color online) Contour plot of the finite-frequency Fano factor $F^{(2)}(\omega)$ as a function of magnetic flux Φ and frequency ω. Colors white, red, and blue correspond to Poissonian, super-Poissonian, and sub-Poissonian values, respectively. Large super-Poissonian peaks occur at the zero-frequency limit only. The shot noise also shows a series of inflexion points at a set of frequencies corresponding to the energy differences ΔE_{ij} of the Hamiltonian (dotted lines). Same parameters as in Fig. 3 with all $t_{ij}=\Gamma$.

In Fig. 7, we plot the finite-frequency skewness for several values of magnetic field with symmetric couplings. For zero field and, indeed, in this symmetric case, for $\Phi/\Phi_0 = n/2$, $n=0,\pm1,\ldots$, the skewness shows a sharp super-Poissonian peak at the origin and also a strong super-Poissonian behavior along the symmetry lines of $F^{(3)}$. Away from these values of the magnetic field, the skewness is strongly sub-Poissonian, except for slight super-Poissonian shoulders at intermediate frequencies before the Poissonian value of unity is recovered at high frequency. The fine structure in the skewness arises from resonances between the three frequencies $|\omega|$, $|\omega'|$, and $|\omega-\omega'|$ and the energy differences ΔE_{ij}.
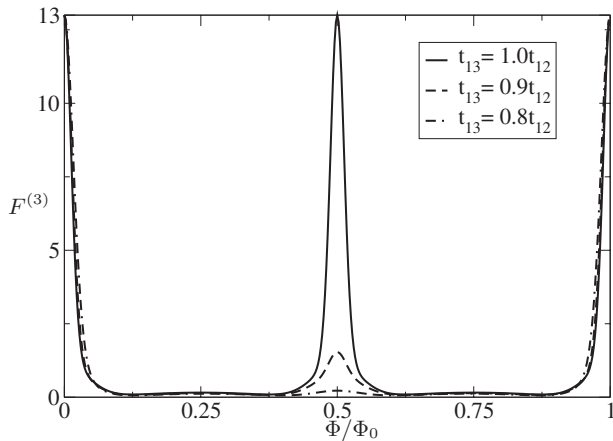

FIG. 6. The zero frequency skewness Fano factor $F^{(3)}(0)$ as a function of flux Φ. The behavior is similar to that of the shot noise, with the highly super-Poissonian maximum value of $F^{(3)}(0)_{\max}=13$. Parameters as in Fig. 4.
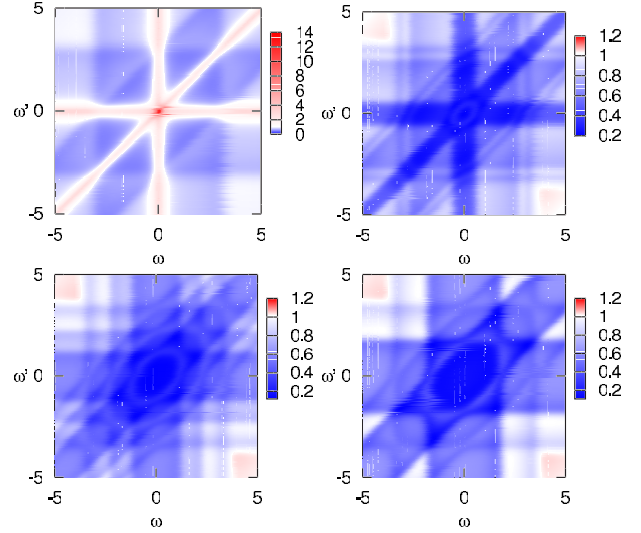

FIG. 7. (Color online) Contour plots of the finite-frequency skewness Fano factor $F^{(3)}(\omega)$ as a function of its two frequency arguments ω and ω' for values of the magnetic flux $\Phi/\Phi_0 = 0, 1/12, 1/6, 1/4$. Parameters and color scheme as in Fig. 5. Strong super-Poissonian behavior only occurs close to $\Phi/\Phi_0 = \frac{n}{2}$; otherwise, the skewness is predominantly sub-Poissonian. The fine structure arises from resonance between the frequencies $|\omega|$, $|\omega'|$, and $|\omega-\omega'|$ and the level splittings of the isolated dot system.

VI. CONCLUSION

The behavior of the coupled triple quantum dot system in a perpendicular magnetic field studied here is governed by the interplay of two quantum-coherent effects: coherent population trapping and the Aharonov-Bohm phase.

We have shown that a dark state, for which no current flows, exists at zero field for arbitrary couplings between the dots, provided t_{13} and t_{23} are both finite. The magnetic field can lift destructive interference, maintaining the dark state, and give rise to oscillations in the current. For arbitrary parameters, the period of these oscillations is Φ_0, but in the special case when the coupling strengths t_{13} and t_{23} are equal the period is halved to $\frac{1}{2}\Phi_0$. These oscillations are also visible in the zero-frequency shot noise and skewness which show large oscillations between strong super-Poissonian and sub-Poissonian behaviors. Finally, at finite frequency, these quantities show a considerable structure, which again shows dramtic dependence of the magnetic field.

APPENDIX: TIME-EVOLUTION MATRIX

The Liouvillian matrix for the system in the basis described just prior to Eq. (3) is

$$\mathcal{L} = \begin{pmatrix}
-2\Gamma & 0 & 0 & \Gamma & 0 & 0 & 0 & 0 & 0 & 0 \\
\Gamma & 0 & 0 & 0 & -2t_{12}\cos\phi & -2t_{13} & 0 & 2t_{12}\sin\phi & 0 & 0 \\
\Gamma & 0 & 0 & 0 & 2t_{12}\cos\phi & 0 & -2t_{23} & -2t_{12}\sin\phi & 0 & 0 \\
0 & 0 & 0 & -\Gamma & 0 & 2t_{13} & 2t_{23} & 0 & 0 & 0 \\
0 & t_{12}\cos\phi & -t_{12}\cos\phi & 0 & -\gamma & 0 & 0 & 2\Delta & t_{23} & -t_{13} \\
0 & t_{13} & 0 & -t_{13} & 0 & -\Gamma/2-\gamma & t_{12}\sin\phi & t_{2,3} & -\Delta+\epsilon & -t_{12}\cos\phi \\
0 & 0 & t_{23} & -t_{23} & 0 & -t_{12}\sin\phi & -\Gamma/2-\gamma & t_{13} & -t_{12}\cos\phi & -\Delta+\epsilon \\
0 & -t_{12}\sin\phi & t_{12}\sin\phi & 0 & 2\Delta & -t_{23} & -t_{13} & -\gamma & 0 & 0 \\
0 & 0 & 0 & 0 & -t_{23} & \Delta-\epsilon & t_{12}\cos\phi & 0 & -\Gamma/2-\gamma & t_{12}\sin\phi \\
0 & 0 & 0 & 0 & t_{13} & t_{12}\cos\phi & \Delta-\epsilon & 0 & -t_{12}\sin\phi & -\Gamma/2-\gamma
\end{pmatrix}$$

$$\text{(A1)}$$

[1] Y. Aharonov and D. Bohm, Phys. Rev. **115**, 485 (1959).

[2] A. G. Aronov and Yu. V. Sharvin, Rev. Mod. Phys. **59**, 755 (1987).

[3] R. G. Chambers, Phys. Rev. Lett. **5**, 3 (1960); A. Tonomura, T. Matsuda, R. Suzuki, A. Fukuhara, N. Osakabe, H. Umezaki, J. Endo, K. Shinagawa, Y. Sugita, and H. Fujiwara, *ibid.* **48**, 1443 (1982).

[4] R. A. Webb, S. Washburn, C. P. Umbach, and R. B. Laibowitz, Phys. Rev. Lett. **54**, 2696 (1985).

[5] A. Yacoby, M. Heiblum, V. Umansky, H. Shtrikman, and D. Mahalu, Phys. Rev. Lett. **73**, 3149 (1994).

[6] Ji Yang, Yunchul Chung, D. Sprinzak, M. Heiblum, D. Mahalu, and H. Shtrikman, Nature (London) **422**, 415 (2003).

[7] A. Yacoby, M. Heiblum, D. Mahalu, and H. Shtrikman, Phys. Rev. Lett. **74**, 4047 (1995).

[8] R. Schuster, E. Buks, M. Heiblum, D. Mahalu, V. Umansky, and H. Shtrikman, Nature (London) **385**, 417 (1997).

[9] A. W. Holleitner, C. R. Decker, H. Qin, K. Eberl, and R. H. Blick, Phys. Rev. Lett. **87**, 256802 (2001).

[10] R. D. Parks and W. A. Little, Phys. Rev. **133**, A97 (1964).

[11] D. Yu. Sharvin and Yu. V. Sharvin, Pis'ma Zh. Eksp. Teor. Fiz. **34**, 285 (1981); **34**, 272 (1981).

[12] V. Chandrasekhar, M. J. Rooks, S. Wind, and D. E. Prober, Phys. Rev. Lett. **55**, 1610 (1985).

[13] B. L. Al'tshuler, A. G. Arnov, and B. Z. Spivak, Pis'ma Zh. Eksp. Teor. Fiz. **33**, 101 (1981); JETP Lett. **33**, 94 (1981).

[14] B. Michaelis, C. Emary, and C. W. J. Beenakker, Europhys. Lett. **73**, 677 (2006).

[15] G. Alzetta, A. Gozzini, L. Moi, and G. Orriols, Nuovo Cimento Soc. Ital. Fis., B **36**, 5 (1976).

[16] E. Arimondo and G. Orriols, Lett. Nuovo Cimento Soc. Ital. Fis. **17**, 333 (1976).

[17] R. M. Whitley and C. R. Stroud, Phys. Rev. A **14**, 1498 (1976).

[18] C. W. Groth, B. Michaelis, and C. W. J. Beenakker, Phys. Rev. B **74**, 125315 (2006).

[19] C. Emary, D. Marcos, R. Aguado, and T. Brandes, Phys. Rev. B **76**, 161404(R) (2007).

[20] A. Vidan, R. M. Westervelt, M. Stopa, M. Hanson, and A. C. Gossard, Appl. Phys. Lett. **85**, 3602 (2004).

[21] L. Gaudreau, S. A. Studenikin, A. S. Sachrajda, P. Zawadzki, A. Kam, J. Lapointe, M. Korkusinski, and P. Hawrylak, Phys. Rev. Lett. **97**, 036807 (2006).

[22] D. Schröer, A. D. Greentree, L. Gaudreau, K. Eberl, L. C. L. Hollenberg, J. P. Kotthaus, and S. Ludwig, Phys. Rev. B **76**, 075306 (2007).

[23] M. C. Rogge and R. J. Haug, arXiv:0707.2058 (unpublished).